SAND2008-1614C

POST-CMOS COMPATIBLE ALUMINUM NITRIDE RING WAVE GUIDE (RWG) RESONATORS

K. E. Wojciechowski, R. H. Olsson III and M. R. Tuck

Sandia National Laboratories, Albuquerque, NM, USA

ABSTRACT

This work presents a new type of MEMS resonator based on launching an acoustic wave around a ring. Its maximum frequency is set by electrode spacing and can therefore provide a means for developing resonators with center frequencies in the GHz. In addition since the center frequency is dependent on the average radius it is not subject to lithographic process variations in ring width. We have demonstrated several Ring Waveguide (RWG) Resonators with center frequencies at 484 MHz and 1 GHz. In addition we have demonstrated a 4th order filter based on a RWG design.

INTRODUCTION

For MEMS devices to be incorporated into RF systems it is desirable to provide CMOS compatible MEMS filters with multiple high frequencies (GHz) and low insertion loss (50Ω impedance). This has yet to be accomplished however great strides are being made in this area [1-6]. One of the limiting factors to developing devices at GHz frequencies is the need to create half-wavelength device features (usually several microns). Recent piezoelectric MEMS devices are employing a method to selectively transduce device harmonics/overtones through use of electrode spacing to determine device harmonic selected. This method has been used by the harmonic contour mode devices proposed and demonstrated in [1,2]. In these devices the mechanical structure can be many times larger than the desired wavelength. Therefore resonator size and hence power handling can be controlled independently of resonant frequency.

Ring waveguide resonators are similar to Surface Acoustic Wave (SAW) devices where lithographically defined electrode spacing, w_E, and average ring radius, R_{avg}, determine the resonator center frequency (Fig. 1). In fact RWG device resonances are created by acoustic wave propagation around the ring. The dependence on average ring radius and electrode spacing enables accurate control of the RWG center frequencies when compared to contour-mode devices [1,3,4,6] where the size mechanical structure determines the center frequency. Additionally, since smaller feature size can be achieved lithographically on metal, higher frequency devices are easier to realize with these resonators. Unlike SAW resonators, which require exotic substrates, and cannot be easily integrated with CMOS processes the RWG devices presented in this work have been fabricated in a post-CMOS compatible aluminum nitride process [1]. Devices implemented in this process are isolated from the substrate by trench isolation (Figure 2). Hence, they are expected to have less loss than typical SAW devices. Finally, the RWG resonator adds an additional degree of freedom in the resonator design as resonances set by electrode spacing, and average radius, can be combined with contour modes set by ring width, w_R. Most importantly, these resonances can be independently tuned. This creates a direct path to the implementation of multi-pole filters.

Two different size RWG resonators have been demonstrated. The first device has an average radius, of 260 μm and a center frequency of 484 MHz (Figure 3). It has a loaded Q of 746 and its motional impedance is 474 Ω. The second device (R_{avg} = 120 μm) center frequency is 998 MHz with a Q = 363 and motional impedance of 2.69 kΩ (Table 1).

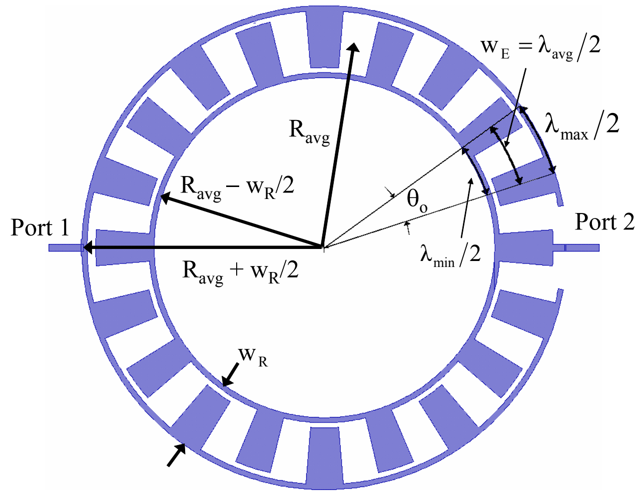

Figure 1: Schematic of ring wave guide resonator electrode configuration. Acoustic wave propagation is around the ring.

DEVICE THEORY

In this section we develop a simple analytical model for the device based on Figure 1. The acoustic wave propagating around the center of the ring has a wavelength, λ_{avg}.

$$\lambda_{avg} = 2R_{avg}\theta_o \quad (1)$$

The nominal center-to-center electrode spacing is $\lambda_{avg}/2$ and the angle at which the electrode configuration repeats is θ_o. This leads to a device resonant frequency of:

$$f_o = \frac{c_R}{2R_{avg}\theta_o} \quad (2)$$

Where c_R is the speed of the material, and is determined by the effective density and stiffness of resonator. This can be estimated from the film thickness of the aluminum nitride (AlN), oxide and metal electrodes. Since the resonant frequency is dependent on the average radius, process variation of the outer and inner radius does not affect it. Note that the number of electrodes, N_e, must be even (3). If this constraint in not followed there will be a discontinuity in the electrodes which may cause unwanted spurious modes.

$$N_e = \frac{\pi}{\theta_o} = \text{even integer} \quad (3)$$

Multiple Modes

Multiple modes can be transduced in the RWG since the average distance between the center of its electrodes varies (Figure

1). In fact the range of wavelengths that can exist in the wave guide is bounded by [λ_{min}, λ_{max}].

$$\lambda_{\min} = 2R\left(_{avg} - \frac{W_R}{2}\right)\theta_o, \qquad (4)$$
$$\lambda_{\max} = 2\left(R_{avg} + \frac{W_R}{2}\right)\theta_o$$

Since the mechanical resonances in AlN are fairly high Q we can expect to see separate peaks in the frequency spectrum corresponding to wavelengths in the range of [λ_{min}, λ_{max}]. In addition, due to the electrode configuration, device harmonics at odd multiples of the fundamental wavelengths (electrode spacing) can be supported while even harmonics are suppressed. This is also true for the harmonic contour mode devices [1, 2]. Finally, an analytical model for a similar SAW resonator has been developed in [7].

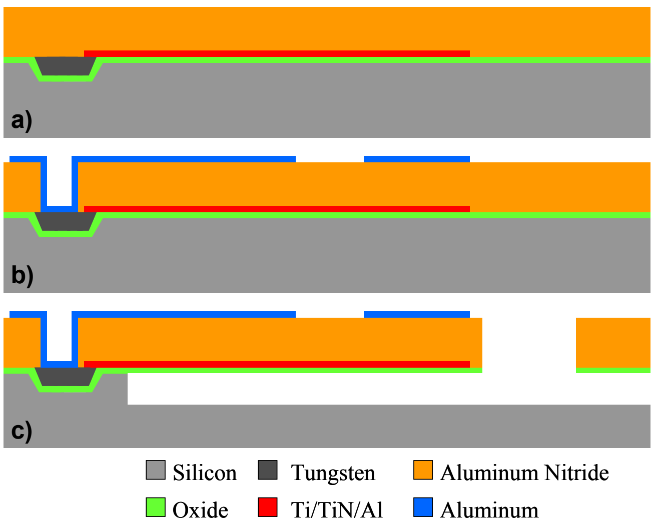

Figure 2: Aluminum nitride microfilter fabrication process.

FABRICATION PROCESS

The process flow used to fabricate the AlN resonators, is shown in Figure 2. The process replaces the platinum bottom electrode in [3] with standard CMOS metals, aluminum (Al), titanium (Ti), titanium nitride (TiN) and tungsten (W). (a) The process begins with an anisotropic silicon (Si) etch and the deposition of a silicon dioxide (SiO_2) layer to isolate the bottom electrode from the substrate. Tungsten is then deposited by chemical vapor deposition (CVD) and chemically mechanically polished (CMP) until it remains only where Si was etched. An oxide touch polish is then performed to further smooth the wafer surface prior to the sputter deposition and patterning of the bottom electrode. The bottom electrode processes utilizes a Ti(20 nm)/TiN(50 nm)/Al(50 nm) bottom electrode. Next, 750 nm of AlN is sputter deposited at 350 ˚C. Using this process highly oriented c-axis AlN films necessary for realizing low impedance resonators can be reliably formed. Typical rocking curve full width half maximum values for the AlN film measured using X-ray diffraction are 1-1.2˚ on Ti/TiN/Al. (b) Contacts to the W areas are etched in the AlN and a 100 nm thick Al top electrode is deposited and patterned. (c) Finally, the resonator frequency is lithographically defined by etching trenches in the AlN and SiO_2 to bulk Si and the devices are released using an isotropic etch in dry SF_6. The maximum temperature in this process is 350 ˚C and all of the materials are post-CMOS compatible and can be deposited and etched using standard CMOS tools.

EXPERIMENTAL RESULTS

Several RWG devices were fabricated. Two of the devices fabricated are shown in Fig. 3. The first device (Figure 3a) has an average radius of 120 µm and angular electrode pitch of 2 degrees. The second device average radius is 260 µm with identical pitch. The resonant frequencies of these devices can be calculated from (2) and are 1022 MHz and 472 MHz respectively (Table 1).

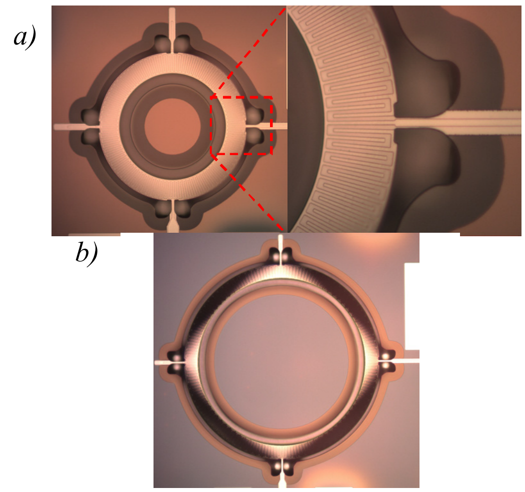

Figure 3: Photomicrographs of RWG resonators, a) Small ring device (R_{avg} = 120µm). b) Large ring device (R_{avg} = 260µm).

Table 1: Parameters of RWG resonators

Parameter	Large Ring	Small Ring
R_{avg}	260 µm	120 µm
Ring width, w_R	40 µm	
θ_o	2 deg	2 deg
$\lambda_{avg}/2$ (electrode spacing)	9.08 µm	4.19 µm
c_R, Material speed (calculated)	8569 m/s	
f_o (calculated)	472 MHz	1022 MHz
f_o (measured)	484 MHz	998 MHz
Insertion Loss (measured)	20.4 dB	34.8 dB
Q	746	363
R_x	474 Ω	2690 Ω
L_x	116.287 µH	155.639 µH
C_x	0.932 fF	0.163 fF
Ring resonator bulk extensional mode	107 MHz	

As can be seen from Table 1 there is close agreement with the calculated and the measured resonant frequencies. The differences are due to AlN thickness variation which results in material speed variation. We are presently working on methods for more accurately controlling AlN film thickness. Figure 4 shows the S21 transmission spectrum for these devices. The small ring device has similar performance to the lateral field excitation device presented in [4].

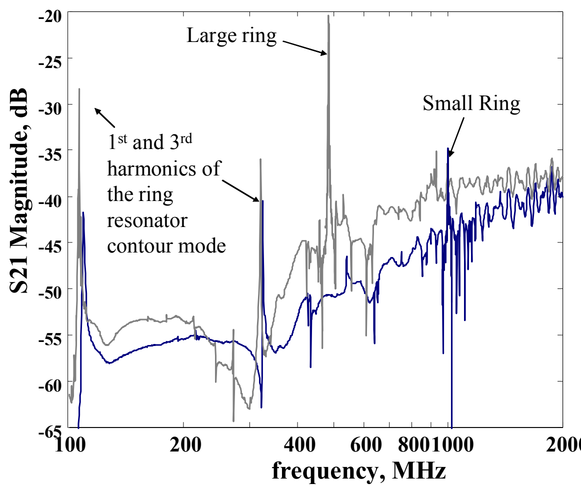

Figure 4: S21 transmission in dB of the large (grey) and small ring (blue) RWG resonators. Note that the contour modes (1^{st} harmonic at 107 MHz and 3^{rd} harmonic at 321 MHz) are present for both rings. Measured in air with an AGILENT E5071C, P_{in} = 0 dBm, Termination = 50Ω.

We also designed a 4^{th} order filter response (Fig. 5) with a RWG filter. It was implemented by placing the ring contour-mode (214MHz) close to the RWG resonance (209MHz) set by the electrode spacing. Since the contour mode is dependent on ring width, w_R, and the average RWG mode is independent of w_R these resonances can be placed close to one another by choosing, w_R and θ_o. This particular RWG filter has an average radius of 120μm and ring width of 20μm. The electrode pitch, w_E, is 20.4μm which corresponds to an electrode angular pitch (θ_E) of 9 degrees.

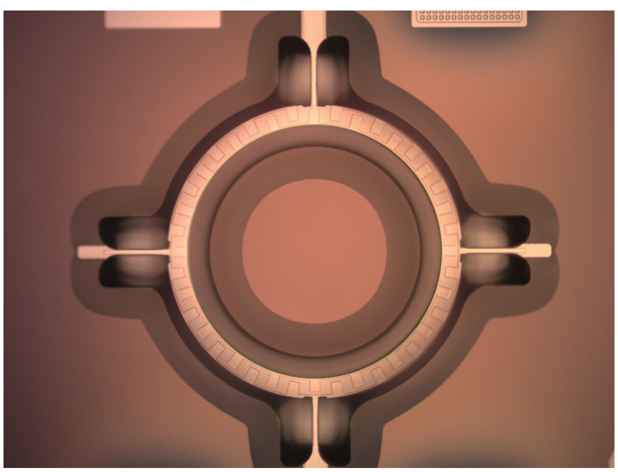

Figure 5: Photomicrograph of a 4^{th} order filter implemented with a combination of contour and RWG modes.

We observed spurious parasitic modes outside the filter band (~200MHz). The cause of these spurious modes and designs to suppress them are being investigated. A differential electrode design could potentially cancel these spurious modes in the filter response.

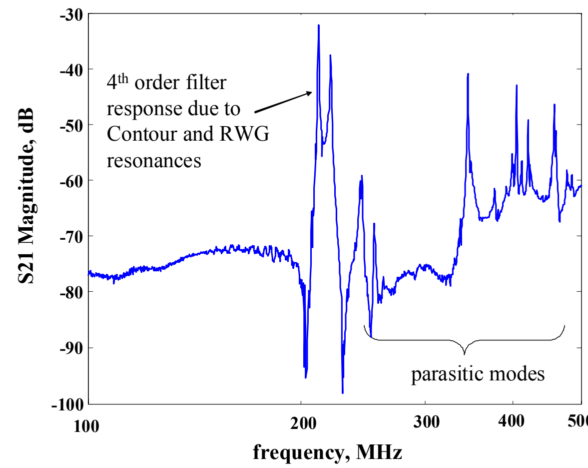

Figure 6: S21 transmission of the 4^{th} order filter realized by combining the 1^{st} harmonic contour-mode of the ring with the SAW like resonance created with the electrode spacing. Measured in air with an AGILENT E5071C, P_{in} = 0 dBm, Termination = 50Ω.

Another interesting result was obtained from a RWG with an electrode angular pitch of 6 degrees, average radius of 120 μm, and width of 40 μm. This shows an example of an RWG exhibiting three modes (Fig. 7) due to the difference in electrode spacing from the inner to outer radius.

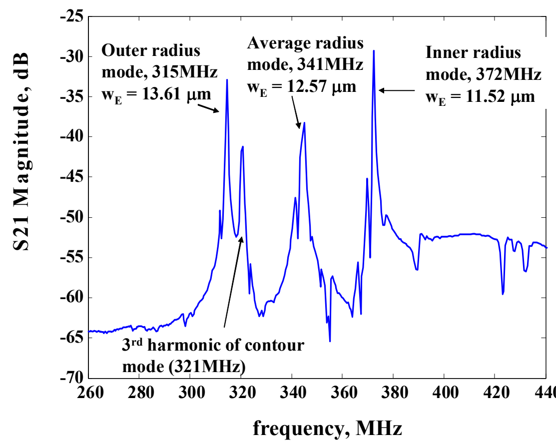

Figure 7: S21 transmission of a RWG resonator where the change in electrode pitch allows for multiple modes to exist. Measured in air with an AGILENT E5071C, P_{in} = 0 dBm, Termination = 50Ω.

Finally, a fully differential large ring device was implemented on a subsequent fabrication run. In this device four electrodes were used to implement a completely differential device. Otherwise it is identical to the device shown in Fig 3a. It was expected to have significantly lower device feed through and lower insertion loss. This was verified by the measured results (Fig. 8). However, unlike the single ended device which exhibited only one mode due to the average radius, the differential device has modes corresponding to the average and inner ring radii. It is not clear why the inner radius mode is present for the differential device while it does not exist in the single ended one. It may be due to the differential drive and sense. Interestingly the outer radius mode is not present and may be suppressed by the anchoring or notching on the outside of the ring. Notching at the anchor, as can be seen in

Figure 3a, was done for stress relief. Finally, with the reduction in the device feed through other modes in the wave guide bandwidth (below -40dB) can be observed in the frequency response of the waveguide (Figure 8).

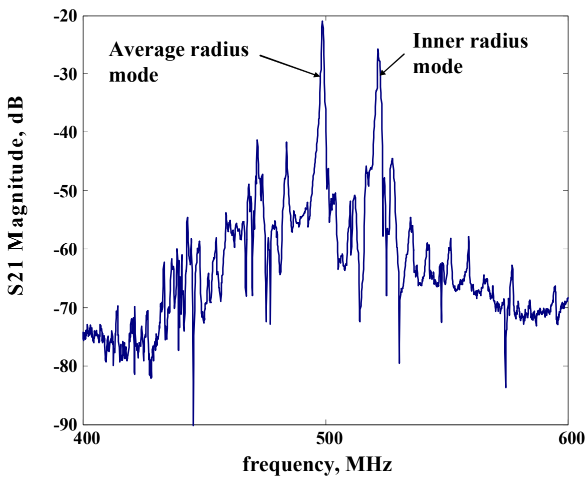

Figure 8: S21 transmission of a fully differential large ring. RWG (260µm average radius, θ_o = 2 degrees). Measured in air with an AGILENT E5071C, P_{in} = 0 dBm, Termination = 50Ω.

CONCLUSIONS

In this work we have presented a RWG device which represents a new type of MEMS resonator. Our first results demonstrate their potential for high-frequency, multi-pole filtering and wide-bandwidth filter implementations in a post-CMOS compatible process. Two RWG resonators have been demonstrated with center frequencies of 484MHz and 1GHz, motional impedances of 474Ω and 2.69 kΩ, and Q's of 746 and 363 respectively. We also demonstrate a 4^{th} order filter response (Figure 6) with a RWG filter implemented by placing the ring contour-mode close to the RWG resonance.

Finally it was experimentally shown that RWG resonators support multiple modes inside the waveguide. This may have possible application in making wide band filters which are difficult to implement with current devices. Additionally, it may be possible to develop multi-pole filters with RWG filters based on electrode configuration alone. This can be achieved by varying electrode pitch around the ring similar to established methods used to achieve multi-pole devices in SAW filters. Alternatively, we could take advantage of the fact that the electrode pitch can be varied from the inner section to the outer section of the ring. With a large enough difference, multiple modes can be excited leading to wider bandwidth filters.

ACKNOWLEDGEMENTS

The authors would like to thank the Microelectronics Development Laboratory staff at Sandia National Laboratories including Jim Stevens and Craig Nakakura for AlN process development. This work was supported by the Laboratory Directed Research and Development program at Sandia National Laboratories. Sandia National Laboratories is a multiprogram laboratory operated by the Sandia Corporation, Lockheed Martin Company, for the United States Department of Energy's National Nuclear Security Administration under contract DE-AC04-94AL85000.

REFERENCES

[1] R. H. Olsson III, J. G. Fleming, K. E. Wojciechowski, M. S. Baker, M. R. Tuck, "Post-CMOS Compatible Aluminum Nitride MEMS Filters and Resonant Sensors," IEEE International Frequency Control Symposium, 2007 Joint with the 21st European Frequency and Time Forum., vol., no., pp.412-419, May 29 2007-June 1 20.

[2] P. J. Stephanou, A. P. Pisano, "PS-4 GHZ Contour Extensional Mode Aluminum Nitride MEMS Resonators," Ultrasonics Symposium, 2006. IEEE , vol., no., pp.2401-2404, 2-6 Oct. 2006.

[3] G. Piazza, P. J. Stephanou, A. P. Pisano, "Single-Chip Multiple-Frequency AlN MEMS Filters Based on Contour-Mode Piezoelectric Resonators," Journal of Microelectromechanical Systems, vol.16, no.2, pp.319-328, April 2007.

[4] J. Wang, J. E. Butler, T. Feygelson, , C. T-C. Nguyen, "1.51-GHz nanocrystalline diamond micromechanical disk resonator with material-mismatched isolating support," *Micro Electro Mechanical Systems, 2004. 17th IEEE International Conference on. (MEMS)* , vol., no., pp. 641-644, 2004.

[5] D. Weinstein, S. A. Bhave, "Internal dielectric transduction: optimal position and frequency scaling," *IEEE Transactions on Ultrasonics, Ferroelectrics and Frequency Control,* vol.54, no.12, pp.2696-2698, December 2007

[6] B. Bircumshaw, G. Liu, H. Takeuchi, T.-J. King, R. Howe, O. O'Reilly, A. P. Pisano, "The radial bulk annular resonator: towards a 50Ω RF MEMS filter," TRANSDUCERS, 12th International Conference on Solid-State Sensors, Actuators and Microsystems, , 2003 , vol.1, no., pp. 875-878 vol.1, 8-12 June 2003.

[7] S. V. Biryukov, G. Martin, M. Weihnacht, "Closed Regular Electrode Structure for SAW Resonators," IEEE International Frequency Control Symposium, 2007 Joint with the 21st European Frequency and Time Forum., vol., no., pp.168-171, May 29 2007-June 1 2007.